Tectono-metamorphic evolution and petrogenesis of a medium-grade fragment of the Variscan orogen: the Zicavo Metamorphic Complex, Corsica (France)

Lorenzo Dulcetta
Department of Chemical and Geological Sciences, University of Cagliari, Cittadella Universitaria, 09042, Monserrato (CA)
DOI: 10.19276/plinius.2025.01.010

INTRODUCTION

The Corsica-Sardinia block (CSb) represents one of the many preserved Variscan domains across Europe. Even though hundreds of articles were published regarding both the orogenic and pre-orogenic features of the Sardinian part of the CSb, studies on the Variscan Corsica are still fragmented. This lack of detailed information on the Corsica transept led to the usual interpretation that Corsica and Sardinia represented a coherent crustal block throughout the entire Palaeozoic. However, recent data (Faure & Ferrière, 2022) may have shed light on a possible different tectonic and paleogeographic interpretation. In order to put new constraints on the tectono-metamorphic evolution and the petrogenesis within the disjointed Variscan basement of Corsica, the Zicavo Metamorphic Complex (ZMC) has been chosen as the study area due to the absence of detailed pressure (*P*) - temperature (*T*) and geochemical data. As such, a combination of field geology, petrography, geochemistry, and thermodynamic modelling has been employed, and the results have been interpreted in the view of the ZMC evolution and the more regional-scale CSb one, giving a possible new description of the pre-Variscan and Variscan evolution of this segment of the orogen.

FIELD GEOLOGY AND DEFORMATION

The ZMC (Fig. 1a) is a highly heterogeneous metamorphic complex consisting of three tectonic units, from bottom to top: the Orthogneiss Unit, the Leptyno-Amphibolite Unit, and the Micaschist Unit (Dulcetta et al., 2023). They are separated by two NE-dipping, dextral, ductile shear zones (Fig. 1b), characterized by a top-to-the-SE sense of shear.

The Orthogneiss Unit is made up of an ultramylonitic orthogneiss, a mylonitic augen gneiss, and garnet-bearing paragneisses on top of the unit. The ultramylonitic orthogneiss is a leucocratic, banded rock consisting of quartz- and feldspar-rich bands which are oriented following the main foliation. The augen gneiss is a coarse-grained rock with K-feldspar and plagioclase porphyroclasts that evidence a top-to-the-SE sense of shear. On top of both orthogneisses, a thin sequence of garnet-bearing paragneisses, which pass to greyish feldspar-rich paragneisses, occurs. The Leptyno-Amphibolite Unit is a thick metavolcanic sequence formed by interlayered amphibolites and meta-rhyolites. Amphibolites can be massive to banded, wherein banding is evidenced by different plagioclase content. The meta-rhyolites are whiteish foliated rocks with feldspars visible by the naked eye. Within the metavolcanics, lenses of garnet-staurolite micaschists, metaconglomerates and serpentinites can be observed. Finally, the Micaschist Unit is formed by garnet-staurolite and garnet-biotite schists, and garnet-bearing phyllites on top.

The ZMC recorded four deformation phases. The D_1 phase is characterized by the development of a metamorphic foliation whose orientation is now impossible to determine due to the strong overprinting and transposition by the subsequent phases. In the Leptyno-Amphibolite and Micaschist Units, the S_1 is highlighted by transposed metamorphic layers of quartz- and/or phyllosilicate-rich composition. In the Orthogneiss Unit, the D_1 deformation was not preserved/recorded. The D_2 deformation is the main deformation at the scale of the complex. It developed a NE-dipping S_2 axial plane foliation associated with F_2 isoclinal folds and an L_2 object lineation; the S_2 is often associated with a top-to-the-SE sense of shear. Furthermore, the mylonitic foliation on the two tectonic contacts is parallel to the regional S_2. The D_3 deformation was responsible for the development of upright open F_3 folds with rarely associated an S_3 crenulation cleavage, while the D_4 phase locally formed sub-horizontal F_4 folds.

METHODS

More than 200 samples were collected and analysed through the use of *i)* electron microscopy and electron microprobe, and *ii)* Raman spectroscopy. Among them, five samples from the three tectonic units were select-

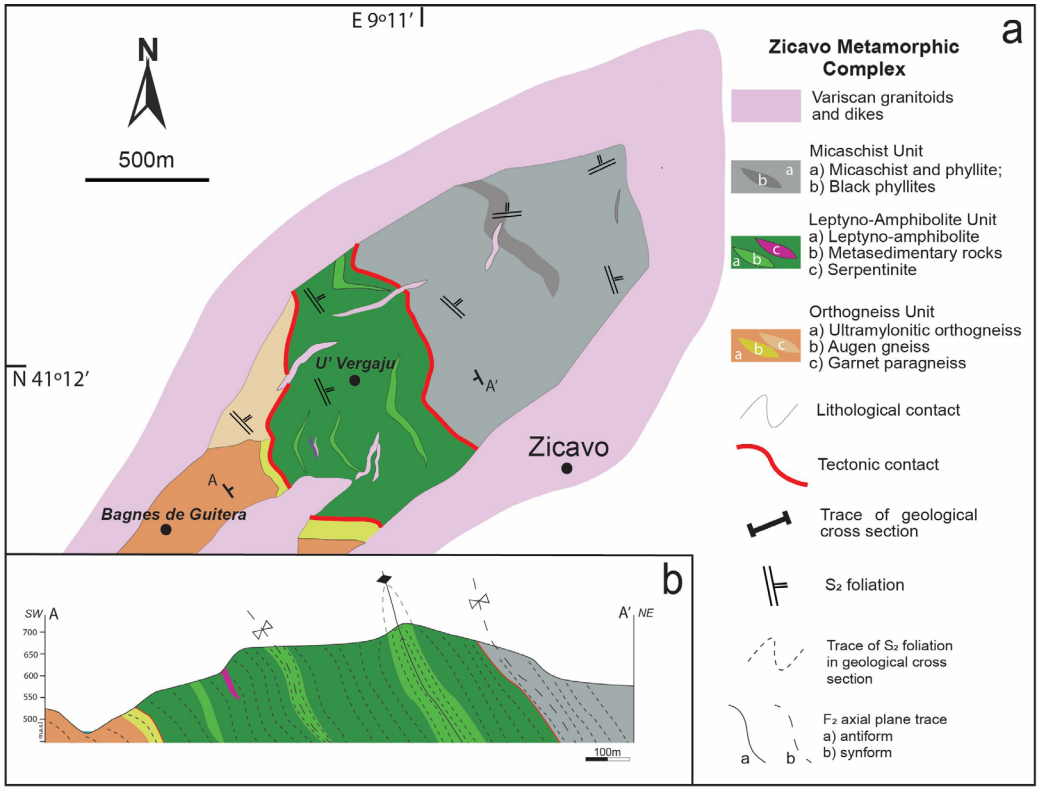

Figure 1 a) *Schematic geological map of the Zicavo Metamorphic Complex.* ***b)*** *Geological cross section of the Zicavo Metamorphic Complex. Modified from Dulcetta et al. (2023).*

ed for detailed thermodynamic modelling and elastic barometry to unravel the metamorphic *P-T* evolution of the ZMC: an augen gneiss from the Orthogneiss Unit, a garnet-staurolite micaschist from the Leptyno-Amphibolite Unit, and three garnet-rich micaschists from the Micaschist Unit. For each modelled sample, *T-X*$^{Fe3+}$ phase diagrams were calculated first to infer a possible amount of ferric iron to be used in the *P-T* phase diagrams' calculations, following petrographic and mineral chemistry information. All diagrams were calculated using the 6.9.1 version of the Perple_X package (Connolly, 1990). The Holland & Powell (2011) internally consistent thermodynamic dataset (the tds633 version), with the Holland et al. (2018) integrated newest *a-X* (activity-composition) solution models, has been used. H_2O-saturation was assumed for all the pelitic samples.

Lastly, 19 selected samples from the Orthogneiss and Leptyno-Amphibolite Units were analysed for their major and trace/REE whole rock compositions by X-ray fluorescence and LA-ICPMS for palaeotectonic inferences.

RESULTS AND DISCUSSION

Petrography and microstructures of selected samples

The selected augen gneiss (sample ZIC-139) consists of mm- to cm-sized porphyroclasts of K-feldspar and (rarer) albitic plagioclase floating in a mylonitic matrix. The porphyroclasts are deformed by a top-to-the-SE sense of shear evidenced by asymmetric mantles and pressure shadows. The matrix is formed by Qz + Kfs + Ab + K-rich Wmca (abbreviations from Warr, 2021) oriented following the S_2 foliation.

Sample ZIC-157 from the Leptyno-Amphibolite Unit is a garnet-staurolite micaschist (Fig. 2a). It consists of Qz + Wmca + Grt + St + Bt + Ilm + And (±Pl±Ap±Mnz). Garnet forms subhedral porphyroblasts which can reach millimetric dimensions; it contains S_1-oriented mineral inclusions of Chl + Wmca + Ilm (±Ap±Qz±Mnz±Zrn±Als). In the matrix, white mica, biotite, ilmenite and staurolite are present. White mica forms very thin prismatic and/or acicular crystals, which are cross-cut by later, coarser mica grains; in between the white mica bundles, trails of biotite are also identified, often retrogressed in chlorite. Moreover, relict paragonite has sometimes been observed together with oriented muscovite, or statically overgrowing the matrix. Staurolite forms subhedral to euhedral prismatic crystals, showing white mica and ilmenite inclusions. Staurolite grows in clusters or single crystals around large garnet porphyroblasts in correspondence with resorption gulfs, in turn with overgrowths of andalusite or chlorite. The matrix is extensively overgrown by post-kinematic, subhedral andalusite, associated with newly formed, highly chloritized, biotite aggregates. Andalusite porphyroblasts grew at the expense of staurolite, muscovite and chlorite, which can sometimes be observed as relict inclusions, while margarite is observed growing along polygonal fractures.

The three samples from the Micaschist Unit (ZIC-3, 10, 11) are, respectively, a garnet phyllite, a garnet-biotite schist and a garnet-staurolite micaschist. The phyllite is a fine-grained rock consisting of Qz + Bt + Wmca + Chl + Grt + Ilm (±Pl±Ap±Zrn±Mnz). Garnet is the main porphyroblast, even though it has sub-millimetric size. It is anhedral to subhedral with pre- to inter-kinematic

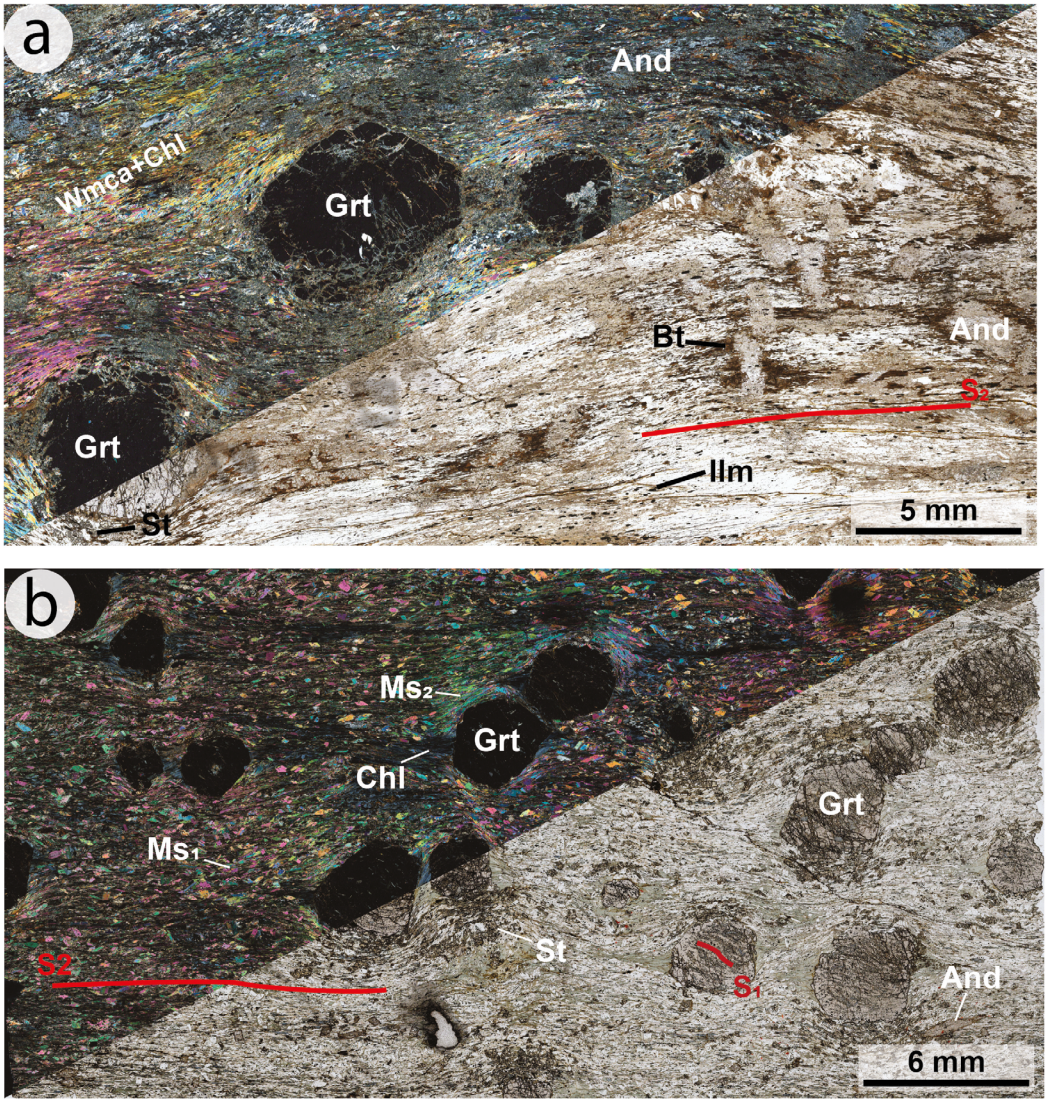

*Figure 2 a,b) Crossed polarized (upper left) and plane-polarized (lower right) photomicrographs for the garnet-staurolite mica-schists ZIC-157 **(a)** and ZIC-11b **(b)**.*

Chl + Qz + Ilm mineral inclusions, and is wrapped by a mica-rich matrix formed by muscovite, chlorite, biotite, quartz and rare plagioclase. The Grt-Bt schist consists of Qz + Pl + Bt + Wmca + Grt + Ilm (±Chl±Ap±Mnz±Zrn). The schists are texturally arranged in alternated layers and/or boudins made up of recrystallized quartz and layers consisting of phyllosilicates, plagioclase, garnet and quartz. Plagioclase represents the main porphyroblast, reaching millimetric size and showing a well-developed compositional zoning. The second main porphyroblast is garnet, which grows as millimetric crystals with equidimensional to elongated shape. It has S_1-oriented mineral inclusions of Qz + Chl + Ilm (±Ep±Zrn). The garnet inclusions' patterns are witnesses of the previous S_1 foliation, which can also be observed in microlithons outside porphyroblasts. Both plagioclase and garnet are wrapped by the S_2-oriented matrix consisting of Bt + Wmca + Ilm ± Chl. In the matrix, biotite has a coarse-grained size and is arranged in trails or aggregates, while white mica is organized either in trails or in mm-thick bundles. Chlorite is mostly a late phase growing on biotite or observed as an inclusion in garnet and plagioclase. The Grt-St micaschist (Fig. 2b) is a coarse-grained, strongly foliated rock made up of Qz + Pl + Grt + Wmca + Chl + St + Bt + Ilm. They are arranged in an oriented matrix, made up of Wmca + Bt + Chl + Ilm, which wraps mm-sized porphyroblasts and quartz-rich boudins. Garnet occurs as poikiloblasts reaching up to 5 mm in diameter. It shows inclusion-rich cores and mantles, and inclusion-poor rims. Inclusions are mainly represented by low amounts of rutile and chloritoid. Ilmenite is abundant in the mantle. In fact, rare rutile in the mantle has been observed overgrown by newly formed ilmenite. White mica is less abundant within garnet. Staurolite is the second main porphyroblast and can reach millimetric sizes, growing at the expense of chloritoid. Clusters of staurolite can also be observed close to the garnet boundaries. The matrix mainly consists of white mica, chloritoid, chlorite, ilmenite, and subordinate quartz, plagioclase, biotite, apatite and monazite.

P-T estimates

Figure 3a shows the *P-T* paths obtained for the five selected samples after detailed *T-X*$^{Fe3+}$ and *P-T* phase equilibrium modelling. Overall, the reported *P-T* conditions show a wide range of pressure and temperature values, especially for the high-pressure (H*P*) stage, both considering the samples' single *P-T* ellipses and/or those of different samples from the same unit.

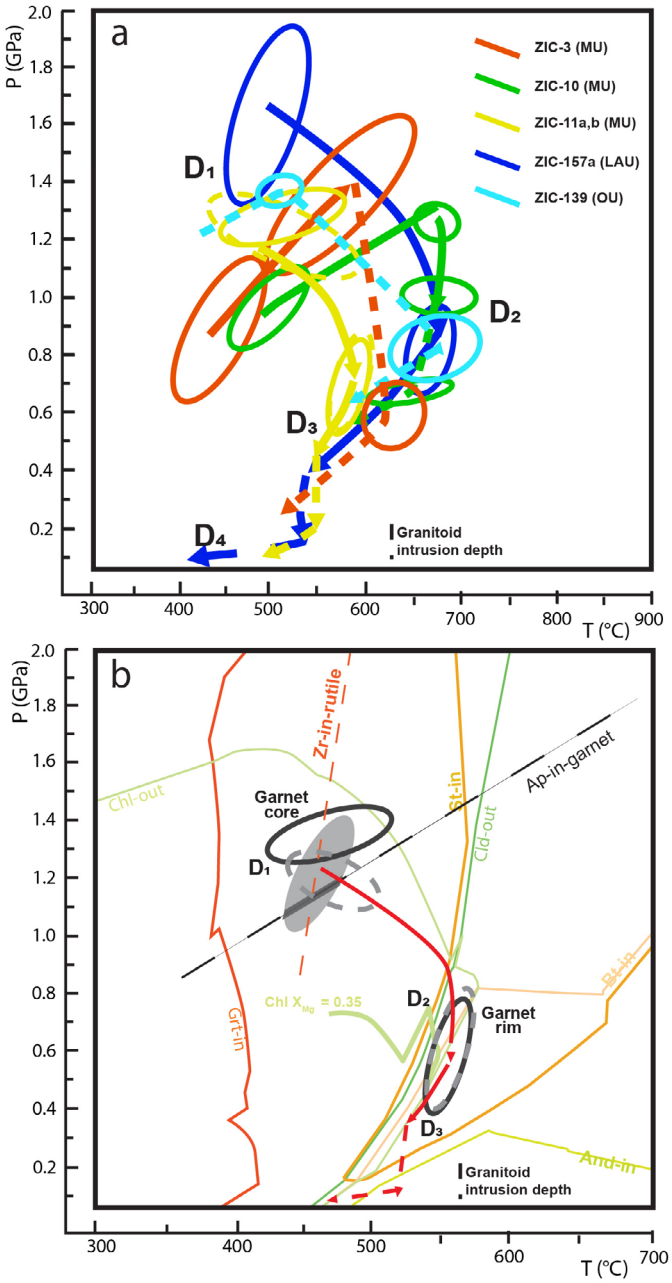

Figure 3 a) *obtained P-T-D metamorphic paths for the selected samples from the Zicavo Metamorphic Complex.* ***b)*** *P-T path for sample ZIC-11 from the Micaschist Unit refined using Zr-in-ritile thermometry and apatite-in-garnet elastic barometry.*

Regarding errors within the single ellipses, this is due to *i)* the propagated errors derived from the thermodynamic modelling, *i.e.*, those errors associated with activity composition models and the thermodynamic database, or *ii)* chemical re-equilibration and component diffusion, which lead to isopleths' scattering. Altogether, the presented *P-T* paths have a similar evolutionary trend. All the modelled rocks underwent a (relatively) high-pressure/low- to medium-temperature metamorphic stage, followed by a rather strong decompression characterized either by heating or isothermal conditions. The pressure and temperature range for the first metamorphic stage falls in the range 0.65-1.9 GPa/400-700°C. The H*P* stage can be said to be coeval to the first deformation phase D_1, which is retained as inclusions' patterns in garnet cores and mantles.

As a whole, the H*P* metamorphic stage in the ZMC, coeval (at least for the pelitic samples) with the first documented D_1 deformation, occurred at relatively high pressures and low to medium temperatures, in a tectonic regime characterized by low geothermal gradients ranging from 9 (ZIC-157a) to 16 (ZIC-10) °C/km. According to the reported *P-T* conditions, the studied samples were buried (assuming a geobaric gradient of 0.03 GPa/km) to depths of 30 (ZIC-3), 40 (ZIC-10), 43 (ZIC-11a,b), and 56 (ZIC-157a) kilometres during the D_1 deformation. These depths, related to the low geothermal gradients, are characteristic of cold subduction environments, or perhaps of the deepest portion of an accretionary prism close to the subducting, cold lithosphere. The inferred *P-T* conditions increase from the shallowest to the deepest rock units. The high-pressure D_1 stage was followed by a rather strong decompression, which indistinctly affected all three units to various degrees. This medium-pressure/medium-temperature (M*P*/M*T*) metamorphic stage has been constrained using the garnet rim and the matrix minerals' isopleths. The matrix minerals are oriented following the main S_2 foliation, which, in the ZMC, is related to a strong, dextral, top-to-the-SE shear deformation. Therefore, this stage was probably coeval with the progressive and composite D_2 deformation phase. The *P-T* conditions for this phase range between 0.65-1.1 GPa/560-720°C. Respectively, the Leptyno-Amphibolite Unit's micaschist, the Micaschist Unit's Grt-St and Grt-Pl micaschists and the Orthogneiss Unit's augen gneiss underwent 25 km, 15 km, 10 km and 18 km of exhumation. The maximum heating was experienced by sample ZIC-157a, which passed from 500 to 650-700°C, just a bit higher than sample ZIC-139 (530-700°C). Samples ZIC-11a,b underwent only ~100°C of heating. Summing up, the M*P*/M*T* metamorphic stage (coeval to the progressive D_2 shear deformation) developed during a heating-decompression trajectory, from high pressure (greenschist/low pressure blueschist facies) to the lower to upper amphibolite facies. The thermal peak occurred in a high geothermal gradient environment of about 20-22 °C/km. This was probably linked to the ongoing collision and crustal thickening, which led to higher temperatures.

The post-D_2 evolution has been less constrained with respect to the prograde part of the *P-T* paths. However, the retrogression may have followed the same trajectory for the studied samples, starting from the thermal peak in the amphibolite facies towards the greenschist facies. This segment of the *P-T* paths can be ascribed to an additional metamorphic stage which was coeval to the D_3 deformation, affecting the ZMC during early retrograde conditions. It probably was a short-lived stage since a low amount of retrograde minerals, such as chlorite, are observed growing with the S_3 foliation or associated with F_3 microfolds. This might be an indication that

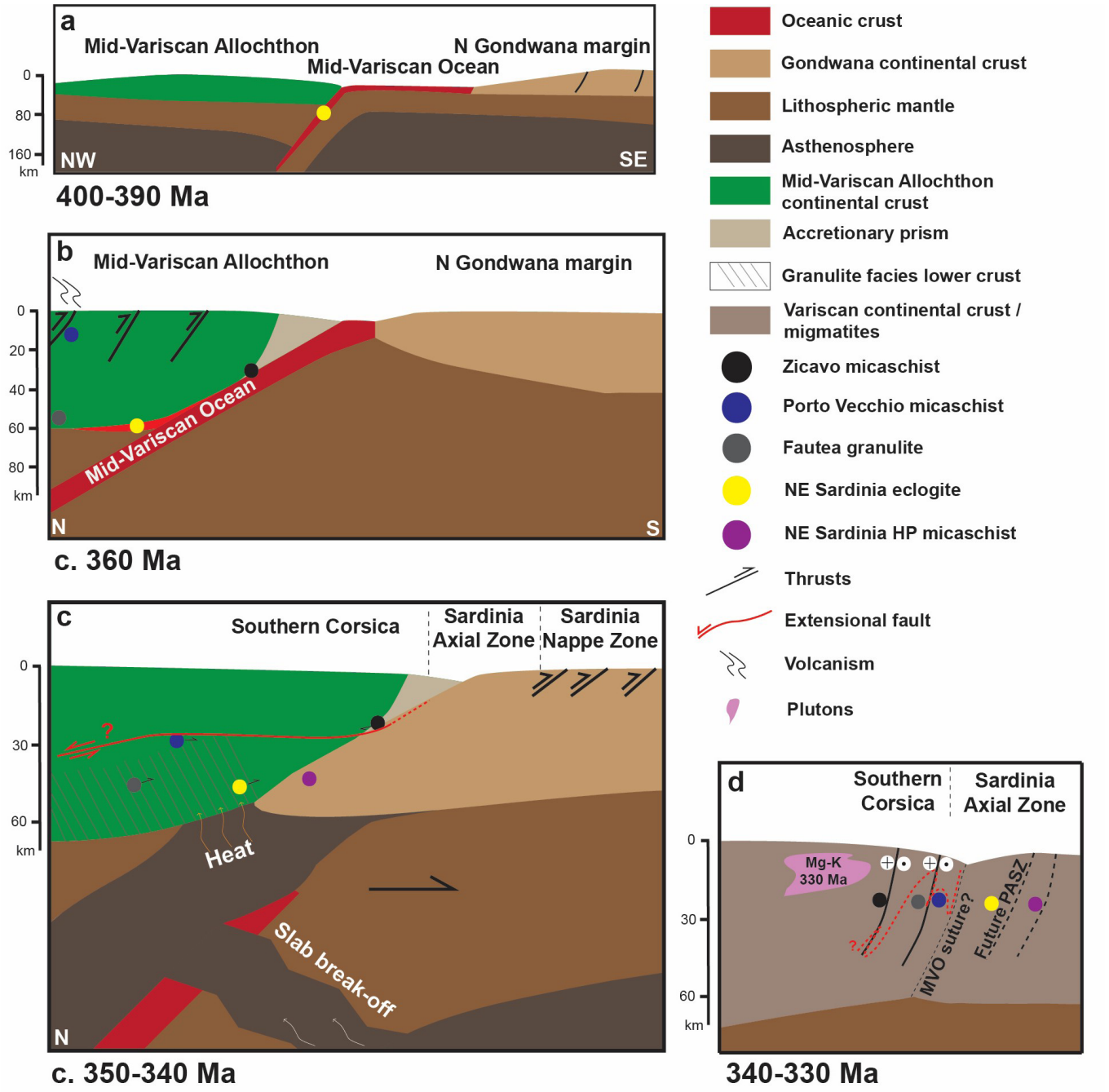

*Figure 4 a-d) Geodynamic evolution from the Devonian **(a)** to the Carboniferous **(d)** for the Corsica and northern Sardinia paleogeographic domains. See details in the text and in Dulcetta et al. (2025).*

there was not enough time to extensively re-equilibrate the rocks according to those conditions. The reason for this apparently short-lived metamorphic stage can be sought in the re-equilibration, after an early retrogression, at high-temperature/low-pressure (*HT-LP*) conditions during the thermal metamorphism that affected the ZMC at various scales. This thermal metamorphic stage occurred at *HT-LP* and is well testified by the staurolite-bearing samples (ZIC-157a and ZIC11a,b), which show widespread, post-kinematic andalusite and biotite blastesis. Contact metamorphism occurred at pressures lower than 0.4 GPa (< 13 km in depth) within the andalusite stability field, at 500°C < *T* < 600°C, since K-feldspar was never observed. Lastly, the HT-LP minerals were partly re-equilibrated and overprinted by later phases, linked to the last and final retrogression, which may be related to a final retrograde stage. These include margarite, paragonite and fine-grained muscovite in the schists, white micas on feldspars, chlorite on biotite, and quartz+chlorite on cordierite. As a whole, the post-thermal peak evolution was characterized by a continuous exhumation due to orogenic collapse, during which the high temperature effect was given by the intruding granitoids. The D_4 deformation, characterized by sub-horizontal folds, probably occurred during these last pulses of the orogenic collapse.

Paleotectonic setting

Major and trace/REE whole rock compositions for the orthogneiss Unit and some metavolcanics from the Leptyno-Amphibolite Unit were plotted on tectonic discrimination diagrams and compared to several other similar rocks across Sardinia and Europe.

The ZMC's Orthogneiss Unit was derived from a peraluminous, calc-alkaline to slightly alkali-calcic, magnesian granite of Middle Ordovician age. Based on the paleotectonic affinity, the Zicavo orthogneiss was set within a volcanic arc part of a convergent setting in Middle Ordovician times. This is coherent with the same tectonic environment of formation of the compared orthogneisses from northern Sardinia and Corsica. However, slight yet remarkable differences can be ascribed from both geochemical and geological points of view. A major difference can be seen in the SiO_2 vs Fe* plot, where the Zicavo orthogneiss clearly shows magnesian features, whereas the Sardinia orthogneisses have ferroan characteristics. Secondly, looking at the spider diagrams, the Zicavo suite is always more enriched in incompatible elements and REE. This feature, and the negative anomalies in Nb and Ta, may imply a lower crustal contamination in the generation of the Zicavo magmas.

The Leptyno-Amphibolite Unit represented a bimodal (basic-felsic) volcanic suite emplaced in pre-Variscan times. The analysed metabasite samples are calc-alkaline basalts to basaltic andesites. Concerning the metarhyolites, they are well plotted within the early extension-related fields, *i.e.*, the within plate fields. Regarding metabasites, they mostly plot in two different fields: a first group plots within fields compatible with a convergent setting of formation, while the second group plots in fields associated with extensional settings. These characteristics may be interpreted to represent a tectonic setting's transition during the emplacement of the entire sequence.

A renewed geodynamic scenario

Amongst the several modelled samples, for which the reconstructed *P-T* paths showed a similar metamorphic evolution, the Grt-St micaschist samples ZIC-11 have been chosen for further *P-T* refinement using trace elements thermometry and apatite-in-garnet elastic barometry. The results are shown in Figure 3b. The details of the work are shown in Dulcetta et al. (2025). The other complexes taken into account are the Fautea and Porto Vecchio ones from Corsica (see Giacomini et al., 2008; Massonne et al., 2018; Cruciani et al., 2021) and the Sardinia eclogites and high pressure micaschists (Cruciani et al., 2012, 2022). Figure 4 shows the presented geodynamic model. The evolution begins in the Lower Devonian with the subduction of the Mid-Variscan Ocean (MVO, Martinez-Catalan et al., 2021) below the Mid-Variscan Allochthon (MVA) (Fig. 4a). Between 365-350 Ma, in Corsica, high-pressure metamorphism was recorded coeval with the D_1 deformation by the Fautea septum's felsic granulites, whereas D_1 high-temperature/low-pressure metamorphism was instead documented by the Porto Vecchio micaschists. These latter rocks were metamorphosed at ~25 km in depth at 362 Ma. Massonne et al. (2018) interpreted this *HT-LP* stage as a metamorphic imprint close to a hot volcanic arc. These features may indicate the position of the Porto Vecchio rocks on the upper plate, that is, the MVA (Fig. 4b). On the other hand, the high pressure recorded by Fautea's felsic granulite may be explained by its position at the base of the upper plate. The high-pressure, syn-D_1 metamorphic stage documented by the ZMC's Grt-St micaschists (Fig. 3a, b) might also be coeval with the D_1 metamorphisms in Fautea and Porto Vecchio. In Sardinia, there is no Variscan *s.s.* metamorphic event before 345-340 Ma. The Zicavo high-pressure rocks may be placed either in the deepest portion of the accretionary prism or in fragments accreted to the base of the upper plate. The former environment seems more likely for the Micaschist Unit's protolith.

Between 350-335 Ma, the Variscan collision began (Fig. 4c). The main metamorphic feature in the ZMC was the extensive amphibolite facies re-equilibration after decompression, exhumation and heating experienced by the three units at different degrees. In Fautea, the felsic granulites underwent their second loop in the granulite facies at > 700°C and 1.0 GPa (~30 km), whereas in Porto Vecchio, the Grt micaschist possibly experienced the metamorphic peak. The decompression and heating during the D_2 must have been linked to *i)* a partial exhumation of the units and *ii)* some kind of heat source. The heat source needs to be sought for also for the granulite facies re-equilibration experienced by the Fautea granulites (and Sardinia eclogites). This heat source may have been given by an asthenosphere upwelling below the MVA, consequence of the slab break off of the descending MVO (Fig. 4c). A coupling between slab break off and lithospheric delamination may also be sought for an even higher thermal regime which explains *i)* the strong, ductile, dextral D_2 shearing at 340 Ma in Corsica, *ii)* the large migmatization at 345 Ma, and *iii)* the tectonic juxtaposition of high-grade metamorphic rocks (*i.e.*, the Fautea rocks) on top of lower-grade rocks (*i.e.*, the ZMC rocks), as it is currently observed. This is shown as a crustal scale normal fault caused by a possible lithospheric delamination below Gondwana, which *i)* brought the Zicavo rocks northward of the Fautea and Porto Vecchio ones, and *ii)* juxtaposed the higher-grade, deeper Fautea granulites and migmatites onto the lower grade, shallower Zicavo and Porto Vecchio complexes. Noteworthy, the D_1 phase in Sardinia is coeval or slightly older than the 335-340 Ma D_2 in Corsica, but considerably younger than the D_1 in Corsica, dated at 360 Ma.

Between 330-320 Ma, the Variscan collision was at its climax. Shear zones such as the East Variscan Shear Zone were probably set on main tectonic features such

as suture zones or former shear zones. In Corsica, after the syn-D_2 dextral shearing, further shear deformation accompanied the development of the D_3 phase at 320 Ma. Meanwhile, in Sardina, the same shearing was active during the D_2 deformation and linked to the activity of the well-known PASZ (Carosi et al., 2020). At this time, the Corsica metamorphic complexes were on their way to the surface after the syn-D_2 thermal peak. Coevally, in Sardinia, the syn-D_2 thermal peak and amphibolite facies metamorphism occurred.

Between Corsica and Sardinia, if they were truly divided already prior to the Variscan collision, a suture should then be present. However, currently there are no witnesses of such a suture that can be clearly recognized, as already pointed out by Faure et al. (2014). In this regard, the rather strong shearing activity that characterized the D_2 and D_3 deformation in Sardinia and Corsica, respectively, might help to constrain a hypothetical position of such a suture. The PASZ and other similar structures across the Variscides have all been related to the evolution of the continental-scale EVSZ. Such a structure had to be imposed on a previous, regional-scale, tectonically weak feature, for instance, a suture zone. Following this interpretation, it may be that between Corsica and Sardinia an oceanic suture lies, now erased and obscured mostly by the EVSZ activity. In light of this evidence, the new presented *P-T* data and upon comparing them with other *P-T* constraints from Corsica and Sardinia, it might have been possible that, before the orogenesis took place, the Variscan rocks of southern Corsica and Sardinia could have belonged to two different paleogeographic domains. Further *P-T*-t, geochemical and geochronological data may help, in the future, to better constrain this scenario.

REFERENCES

Carosi, R., Petroccia, A., Iaccarino, S., Simonetti, M., Langone, A., Montomoli, C. (2020) - Kinematics and timing constraints in a transpressive tectonic regime: The example of the Posada-Asinara Shear Zone (NE Sardinia, Italy). Geosciences, 10(8), 288.

Connolly, J.A.D. (1990) - Multivariate phase diagrams: an algorithm based on generalized thermodynamics. Am. J. Sci., 290, 666-718.

Cruciani, G., Franceschelli, M., Groppo, C., Spano, M.E. (2012) - Metamorphic evolution of non-equilibrated granulitized eclogite from Punta de li Tulchi (Variscan Sardinia) determined through texturally controlled thermodynamic modelling. J. Metamorph. Geol., 30(7), 667-685.

Cruciani, G., Franceschelli, M., Massonne, H.-J., Musumeci, G. (2021) - Evidence of two metamorphic cycles preserved in garnet from felsic granulite in the southern Variscan belt of Corsica, France. Lithos, 380-381, 105919.

Cruciani, G., Franceschelli, M., Carosi, R., Montomoli, C. (2022) - P-T path from garnet zoning in pelitic schist from NE Sardinia, Italy: further constraints on the metamorphic and tectonic evolution of the north Sardinia Variscan belt. Lithos, 428-429, 106836.

Dulcetta, L., Faure, M., Rossi, P., Cruciani, G., Franceschelli, M. (2023) - Geology of the Zicavo Metamorphic Complex, southern Corsica (France). J. Maps, 19(1), 2264320.

Dulcetta, L., Zhong, X., Cruciani, G., Vrijmoed, J., Pleuger, J., Franceschelli, M., John, T. (2025) - Coupling Phase Equilibrium Modelling and Apatite-in-Garnet Elastic Barometry to Unravel the P–T Path of the Micaschist Unit From the Zicavo Metamorphic Complex (Corsica, France). J. Metamorph. Geol., *In Press*.

Faure, M., Rossi, P., Gaché, J., Melleton, J., Frei, D., Li, X., Lin, W. (2014) - Variscan orogeny in Corsica: New structural and geochronological insights, and its place in the Variscan geodynamic framework. Int. J. Earth Sci., 103(6), 1533-1551.

Faure, M. & Ferrière, J. (2022) - Reconstructing the Variscan Terranes in the Alpine basement: Facts and arguments for an Alpidic Orocline. Geosciences, 12(2), 65.

Giacomini, F., Dallai, L., Carminati, E., Tiepolo, M., Ghezzo, C. (2008) - Exhumation of a Variscan orogenic complex: Insights into the composite granulitic–amphibolitic metamorphic basement of south-east Corsica (France). J. Metamorph. Geol., 26(4), 403-436.

Holland, T.J.B. & Powell, R. (2011) - An improved and extended internally consistent thermodynamic dataset for phases of petrological interest, involving a new equation of state for solids. J. Metamorph. Geol., 29, 333-383.

Holland, T.J., Green, E.C., Powell, R. (2018) - Melting of peridotites through to granites: a simple thermodynamic model in the system KNCFMASHTOCr. J. Petrol., 59(5), 881-900.

Martínez Catalan, J.R., Schulmann, K., Ghienne, J.F. (2021) - The Mid-Variscan Allochthon: keys from correlation, partial retrodeformation and plate-tectonic reconstruction to unlock the geometry of a noncylindrical belt. Earth Sci. Rev., 220, 1-65.

Massonne, H.-J., Cruciani, G., Franceschelli, M., Musumeci, G. (2018) - Anticlockwise pressure temperature paths ecord Variscan upper-plate exhumation: Example from micaschists of the Porto Vecchio region, Corsica. J. Metamorph. Geol., 36(1), 55-77.

Warr, L.N. (2021) - IMA–CNMNC approved mineral symbols. Mineral. Mag., 85(3), 291-320.